Dominant Daily Modes of the South Asian Summer Monsoon Rainfall in the NCEP Climate Forecast System

Deepthi Achuthavarier[1,*] and V. Krishnamurthy[1,2]

[1]*Department of Climate Dynamics*
George Mason University, Fairfax, VA
[2]*Center for Ocean-Land-Atmosphere Studies, Calverton MD*

NOAA CTB - COLA
Joint Seminar
April 11, 2008

1. Introduction

Observational studies by Krishnamurthy and Shukla (2007, 2008; KS07 and KS08 hereafter) and Krishnamurthy and Kirtman (2008; KK08, hereafter) have demonstrated that the convective and rainfall anomalies associated with the south Asian summer monsoon consist of two intraseasonal oscillatory modes with periods around 45 and 28 days and two non-oscillatory or persistent components which are related to ENSO and Indian Ocean dipole sea surface temperature (SST). These results are based on a multi-channel singular spectrum analysis (MSSA) of daily anomalies of the observed outgoing long wave radiation (OLR) and rainfall data. The persistent modes are characterized by large scale patterns that prevail over most of the south Asian monsoon region with same sign anomalies throughout the summer monsoon season [June-September (JJAS)]. Their results also show that the seasonal anomalies are largely determined by the amplitude and sign of the persistent modes, emphasizing the role of low frequency variability of SST in climate predictability. Despite this potential, success in seasonal forecasts depends on the ability of the current general circulation models (GCMs) to correctly simulate the above-mentioned modes and their relationship with the SST.

The objective of the present study is to examine and document the dominant daily modes of the summer monsoon rainfall in a state-of-the-art coupled GCM. This study will provide an account of the intraseasonal variability in a coupled model as well as its seasonally persistent components that are shown to be pivotal in understanding the interannual variability of the monsoon. The ENSO-monsoon teleconnection in the model will be discussed from a new point of view opened by the recognition of the seasonally persistent components. The impacts of horizontal resolution and air-sea coupling will also be mentioned briefly at the end.

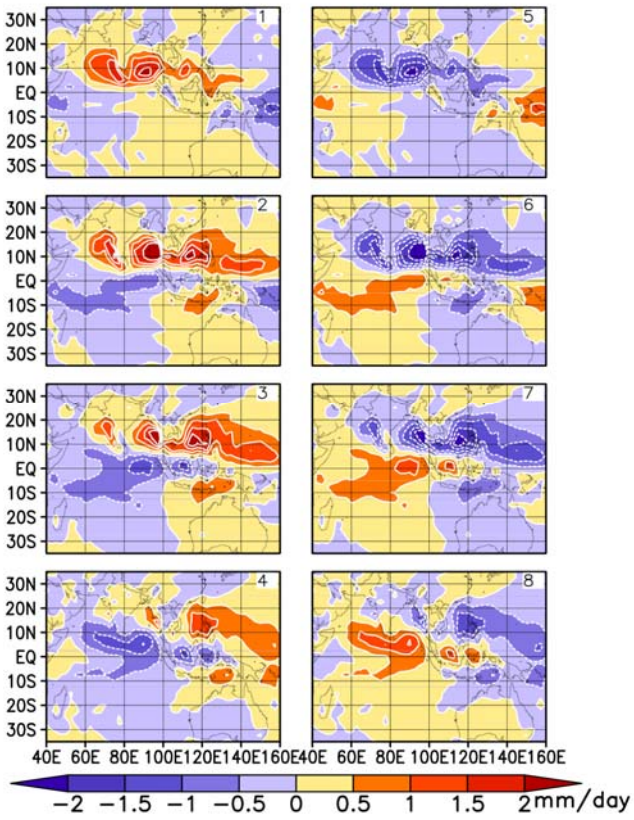

Figure 1 Phase composites of the 100-day oscillatory mode of the CFST62. One cycle is divided into 8 equally spaced intervals. Units are in mm day^{-1}.

2. Models and methods of analysis

2.1 Models

The primary model used in this study is the Climate Forecast System (CFS) with a horizontal resolution of 62 waves, developed at the National Centers for Environmental Prediction (NCEP). The atmospheric component of the CFS is the NCEP's Global Forecast System (GFS) and its ocean component is the Modular Ocean Model version 3 (MOM3) of the Geophysical Fluid Dynamics Laboratory (GFDL). The atmosphere-ocean coupling in the CFS spans from 65°S to 50°N, and

*Correspondence to: Deepthi Achuthavarier, Department of Climate Dynamics, George Mason University, Fairfax, VA; E-mail: deepthi@cola.iges.org

the coupling interval is once a day. No flux correction is employed in the CFS. A detailed description of the model can be found in Saha et al. (2006). Daily mean precipitation data from a 52 year long simulation of the CFST62 (CFS with T62 resolution) (Pegion and Kirtman 2008) is used in this study. In order to examine the impact of horizontal resolution, a 100 year long simulation of the T126 version of the CFS (CFST126) is obtained from the NCEP. Additionally, data from an AMIP (Atmospheric Model Intercomparison Project) type simulation by the GFS is also considered (B. Jha, Personal Communication). The GFS, which is of T62 resolution (GFST62), is run from 1950 to 2002 (53 years) with prescribed monthly reconstructed SST. From all the three simulations, the last 30 years of data are analyzed. The results are compared with observational findings of KS08 and KK08.

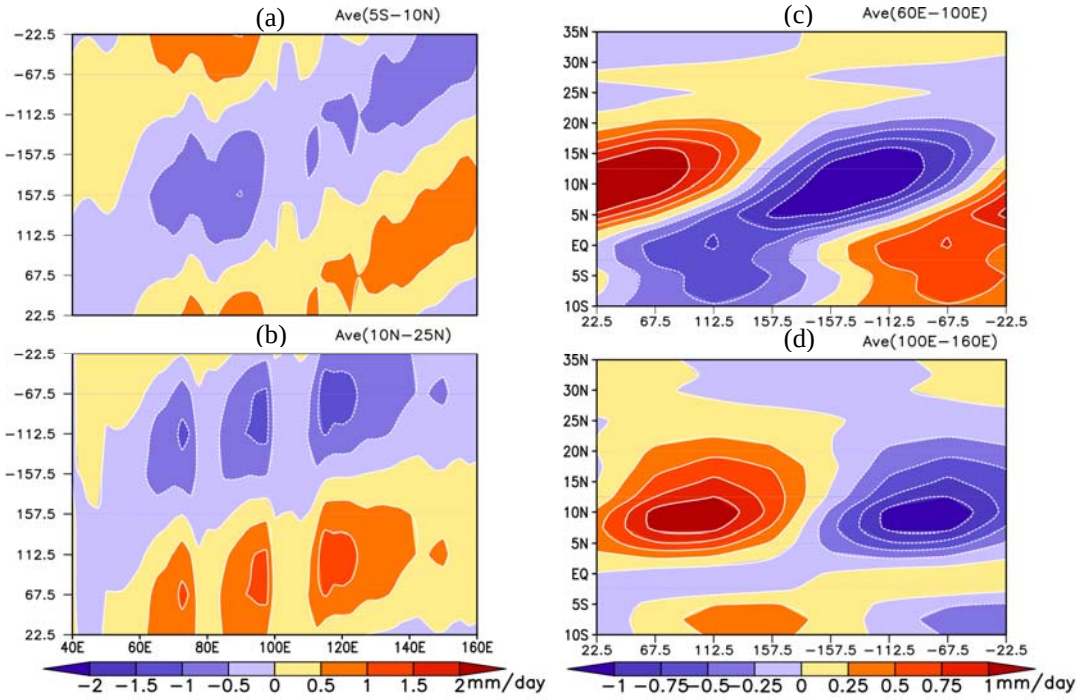

Figure 2 Longitude-time cross sections of the 100-day oscillatory mode of the CFST62 computed by averaging over the latitudes 5°S-10°N (a) and 10°N-25°N (b). Latitude-time cross sections of the 100-day oscillatory mode of the CFST62 computed by averaging over the longitudes 60°E-100°E (c) and 100°E-160°E (d). The y-axis in (a) and (b) and the x-axis in (c) and (d) represent phase angle. Units are in mm day^{-1}.

2.2 Methods

The analysis methods used in this study follow those of KS08. The dominant daily modes of monsoon are obtained by performing an MSSA on daily anomalies of rainfall for the JJAS season. No filters are applied on the data except for a 5-day running mean to remove synoptic scale fluctuations. While a traditional empirical orthogonal function (EOF) analysis provides the spatial patterns of maximum variance, MSSA isolates the spatial structure of the most dominant modes as well as their propagation in time (Plaut and Vautard 1994). In the context of a dynamical system, MSSA can be considered as a tool to isolate quasi-periodic and quasi-stationary orbits of the system. The computational procedure of MSSA can be briefly described as follows. Let the original data set contain L spatial points (channels) at N discrete time intervals. The lagged covariance matrices are constructed by choosing a certain lag window of length M for each L spatial point. The lagged covariance matrices for all spatial points are arranged to form a trajectory matrix of order (LM, N-M+1), eigenanalysis of which yields LM eigenvalues and LM eigenvectors. The eigenvectors contain M sequences of spatial maps and are referred as space-time EOFs (ST-EOFs). The space-time principal components (ST-PCs), each of length N-M+1 are obtained by projecting the original data on to the corresponding ST-EOFs. The component of the original data corresponding to each eigenvalue can be reconstructed by projecting the ST-PC

onto its respective ST-EOF, and is referred as the reconstructed component (RC). The RCs share the spatial and temporal dimensions of the original dataset and can be considered as the filtered data corresponding to a particular mode.

3. Climatology and variability

Preliminary analysis shows that all three simulations (CFST62, CFST126 and GFST62) capture the general features of the JJAS seasonal climatology of rainfall over the south Asian monsoon region (40°E-160°E, 35°S-35°N). A few deficiencies to note are the overestimation of rainfall over the southwestern and northeastern parts of India and the underestimation over the central India, western Pacific and the south China Sea region. An erroneous patch of rainfall anomaly is seen over the western equatorial Indian Ocean in both the coupled models, but is not present in the GFS. The interannual and the intraseasonal variability of the three simulations are examined by computing the standard deviation of the JJAS seasonal and pentad anomalies. Although the models capture the spatial structure of variability, which includes maxima on either side of the Indian peninsula and over the western Pacific and minima over the southeastern parts of India, the amplitude of the variability is considerably overestimated. Comparing between the coupled models, there is no noticeable improvement in the CFST126 as far as the climatology and variability are considered. However, the uncoupled run fails to capture the rainfall maxima over the western Pacific and South China Sea region.

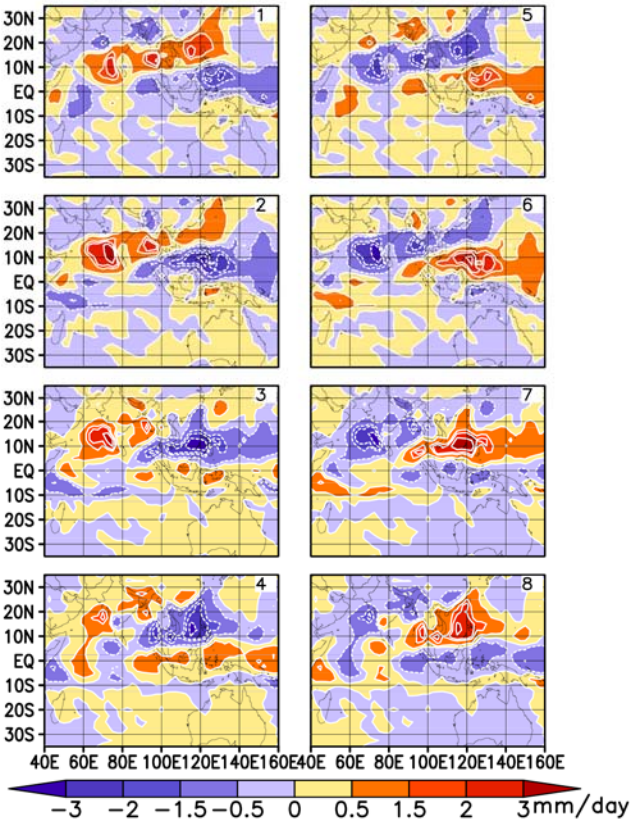

Figure 3 Phase composites of the 30-day oscillatory mode of the CFST62. One cycle is divided into 8 equally spaced intervals. Units are in mm day^{-1}.

4. Dominant daily modes of rainfall in the CFS

Following the observational study of KS08, MSSA with a lag window of 61 days is performed on the daily anomalies of rainfall during the JJAS season for 30 years of model data from CFST62, CFST126 and GFST62. This analysis, which was performed exclusively on the JJAS season in order to isolate the summer modes, yielded only a single pair of intraseasonal modes of 30-day period. A closer examination of the other dominant non-oscillatory modes indicated that the dataset contained another intraseasonal mode probably with a longer period that was not resolved in the lag window used in this analysis. Therefore, a new MSSA was performed taking all days of the year and employing a longer lag window of 181 days. This analysis revealed two pairs of oscillatory modes with periods around 100 days in the coupled models, and a single pair of oscillatory mode of 70-day period in the uncoupled model. Out of the two 100-day modes, one is found to be dominant during the summer and another during the winter season. The winter mode is likely to be the Madden Julian Oscillation (MJO). This study will focus on the two summer modes mentioned above.

4.1 Oscillatory modes

As mentioned above, CFST62 shows two summer intraseasonal modes with periods 100 and 30 days. Figure 1 shows phase composites calculated from the RCs corresponding to the 100-day oscillatory mode. Since the MSSA isolates the oscillatory mode in a pair, RC of such a mode is obtained by adding the corresponding RCs constituting that pair; i.e., RC of 100-day mode, denoted by RC34 is the sum of RCs 3 and 4. Phase angles of the oscillations are calculated from the RCs, following Krishnamurthy and Shukla (2007). One complete cycle

of oscillation is divided into eight intervals that are 45 degrees apart. The phase composite for a particular phase is computed by averaging parts of the RC falling into that particular phase. Figure 1 shows that the anomalies developed over the equatorial Indian Ocean slowly propagate northeastward and develop into a large scale tilted pattern extending from 60°E to 140°E. This large-scale pattern is characteristic of the 45-day mode discussed in KS08 (their Figure 4).

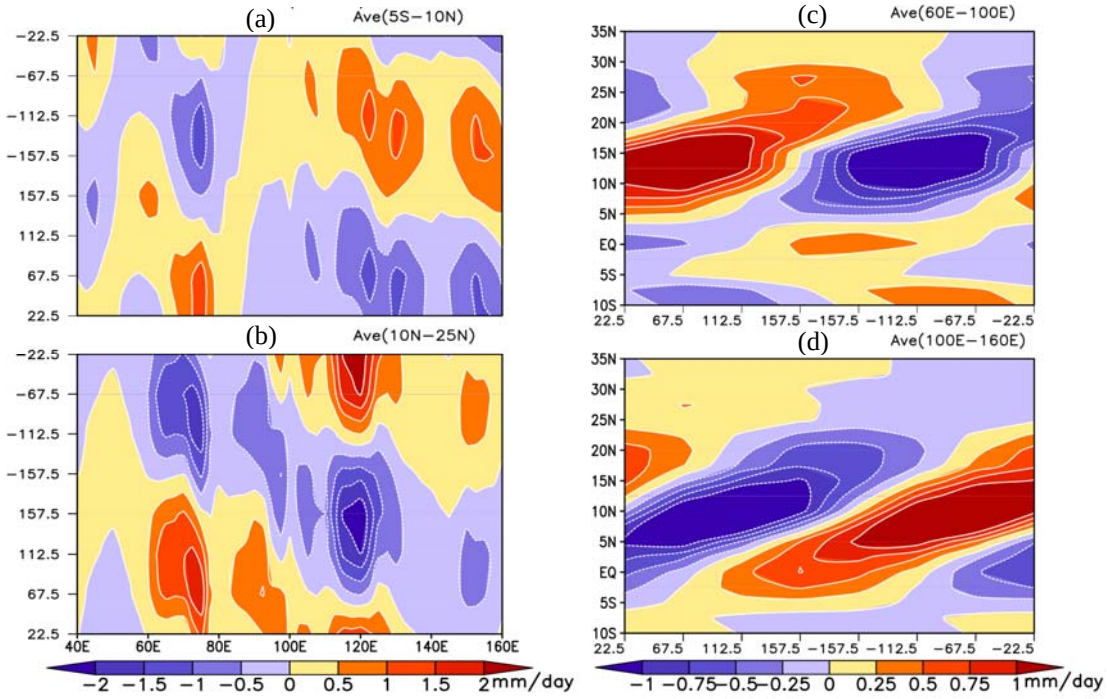

Figure 4 Longitude-time cross sections of the 30-day oscillatory mode of the CFST62 computed by averaging over the latitudes 5°S-10°N (a) and 10°N-25°N (b). Latitude-time cross sections of the 30-day oscillatory mode of the CFST62 computed by averaging over the longitudes 60°E-100°E (c) and 100°E-160°E (d). The y-axis in (a) and (b) and the x-axis in (c) and (d) represent phase angle. Units are in mm day^{-1}.

The propagation characteristics of the 100-day mode are examined by plotting longitude-time and latitude-time cross sections of the phase composites (Figure 2). It is seen that the 100-day mode has coherent eastward propagation between the latitudes 5°S and 10°N and northward propagation from 5°N to 20°N. These results are consistent with the observational findings except for that the model fails to capture northward propagation between 100°E and 160°E (see Figure 10 of KS08). Figures 1 and 2 suggest that the 100-day mode must be equivalent to the 45-day mode obtained in observations. An important point to note here is that, although the model captures the spatial structure and propagation characteristics of the mode, the intraseasonal oscillations in the model are considerably slower and extend well beyond the JJAS summer season. The phase composites and the propagation of the 30-day mode are shown in Figure 3 and 4. The spatial structure of the 30-day mode does not show the characteristic quadruple structure seen in its observational counterpart (see Figure 5 of KS08). However, longitude-time and latitude-time cross sections of the phase composites suggest coherent westward and northward propagation as seen in observations (Figure 4).

The relation between the intraseasonal modes and the SST is examined by computing daily point correlation between RCs averaged over the EIMR (Extended Indian Monsoon Region; covers the area 70°E-110°E, 10°N-30°N) and daily anomalies of the SST. The 100-day mode shows moderate dependence on the eastern Pacific and Indian Ocean SST where correlations values range up to 0.4. The 30-day mode shows little correlation (values below 0.1) with the SST over most of the ocean basins, which suggests that it might be an atmospheric-only mode. These results are consistent with the observations.

4.2. Non-oscillatory or persistent modes

This section examines the persistent components among the first 8 modes obtained from the 181-day-lag-window MSSA. Figure 5 shows the daily point correlation between the EIMR index computed from the RCs of the four persistent modes and daily SST anomalies. The spatial structure of the correlation patterns of the RCs 1, 5 and 8 have an ENSO-like structure in the Pacific and compare well with the correlation map of the observed ENSO mode (see Figure 4(c) of KK08). Daily rainfall anomalies corresponding to the modes 1, 5 and 8 are negatively correlated with the eastern Pacific SST, consistent with the findings of KK08 (their Figure 4(c)). Note that the sign of the correlation is opposite in KK08 since they used the OLR anomalies instead of the precipitation. Thus there are three modes showing possible links with the ENSO, while the observational analysis produced only a single ENSO mode. One explanation could be that, by performing the analysis on the entire data as opposed to only the summer season, the ENSO modes of different timescales might be captured here.

Another important point to note from Figure 5 is that the correlation map for RC2 has a pattern similar to the rest of the modes but with positive correlations over the eastern Pacific. It is not clear whether this is the model equivalent of the dipole mode. However, it is to be noted that this is the second mode resolved in the MSSA and its contribution to the seasonal anomalies is not negligible (Figure not shown).

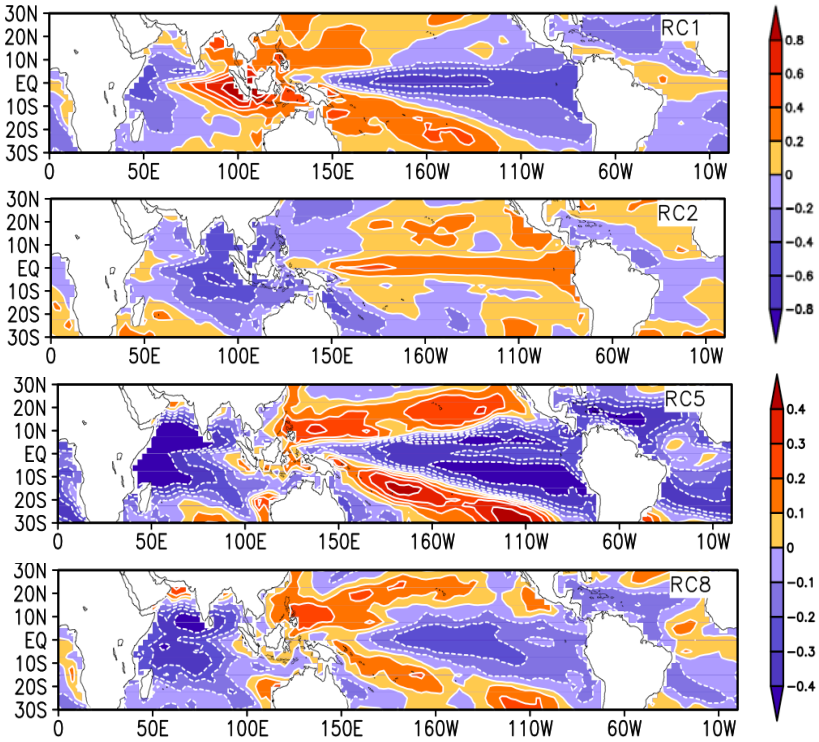

Figure 5 Daily point correlation between the EIMR index computed from RCs 1, 2, 5 and 8 and the daily anomalies of the SST using the CFST62 data. The top color bar applies to RC1 and RC2 and the bottom to RC5 and RC8.

It is widely known among the CFS users that the model has an apparent failure to capture the correct sign of the ENSO monsoon correlation in the interannual time scale. The relation between summer monsoon and the ENSO is often depicted as a lead lag correlation between the JJAS seasonal anomalies of the EIMR index and the monthly anomalies of the NINO3 index. (The NINO3 index is the SST anomalies averaged over the region 150°W-90°W, 5°N-5°S). Observational data show that the correlation between monsoon rainfall and NINO3 index stays close to zero during the months preceding the monsoon, but reaches a maximum of about -0.6 during the winter season following the monsoon season. A similar analysis performed on the CFST62 data produces an unrealistic curve that has positive correlations during and after the monsoon season (Figure 6(a)). The seemingly strange behavior of the RC2 discussed earlier prompted us to examine whether the RC2 offers any explanation for the lack of ENSO-monsoon teleconnection in the model.

Figure 6(b) shows the lead/lag correlation between the JJAS seasonal anomalies of EIMR index calculated from first two persistent modes (RCs 1 and 2) and the 100-day oscillatory mode (RC34) and monthly NINO3 index, all taken from the CFST62 run. The black line in Figure 6(b) represents the lead-lag correlation analysis performed for the total rainfall anomalies of CFST62 and is same as the black line in Figure 6(a). Although the total anomalies fail to capture the correct sign of the correlation, the MSSA mode RC1 captures the observed

ENSO-monsoon relationship. However RC2 and RC34 closely follow the total anomalies. From the above analysis, we would like to emphasize two points: Firstly, although not revealed in the conventional analysis, the CFS does contain a mode, which captures the correct ENSO-monsoon teleconnection in the interannual time scale. Secondly, the positive correlation between seasonal mean rainfall and monthly NINO3 anomalies in the CFS might be linked to other dominant modes such as RC2 and RC34 and their relationships with the SST.

5. Comparison with CFS T126

Two MSSA were performed on the CFST126 data, with lag windows 61 and 181 days, which isolated two summer intraseasonal modes with periods 30 and 100 days. The spatial structure of the oscillatory modes and their correlation with SST did not show any noticeable difference from those of the CFST62. The phase composites and the latitude-time and longitude-time cross sections for the oscillatory modes resembled well with those of the CFST62.

6. Comparison with GFS

The GFS produced two oscillatory modes with periods around 70 days and 30 days. The 70-day mode has clear northward propagation, but incoherent eastward propagation. The 30-day mode has northwestward propagation and is somewhat similar to its counterparts in the coupled models. One noticeable difference seen in the GFS is that none of its dominant persistent modes captured the correct ENSO mode i.e., a mode equivalent to the RC1 in CFST62. This emphasizes the importance of coupled processes in simulating the ENSO-monsoon correlation.

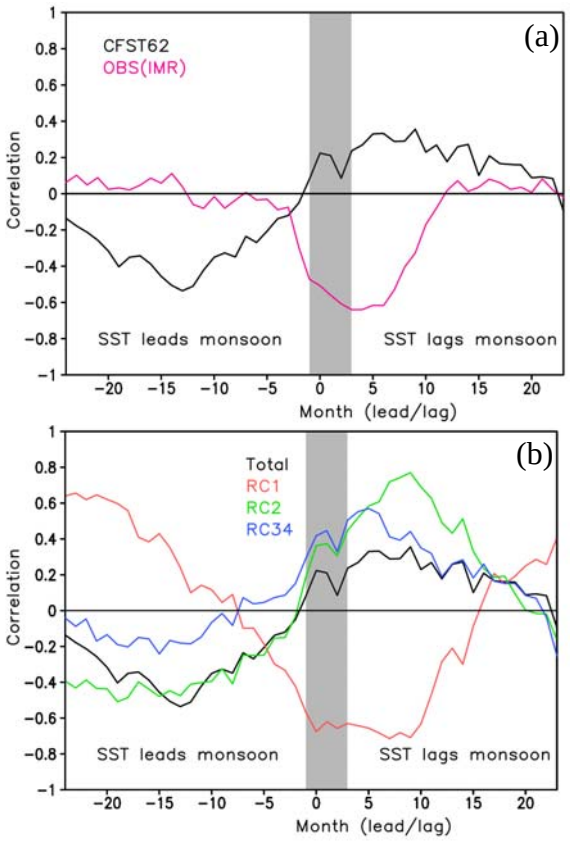

Figure 6 Lead/lag correlation between JJAS seasonal anomalies of the EIMR index and the monthly NINO3 values using the CFST62 data ((a) and (b); black curve). Pink curve in (a) shows similar analysis performed on the observational data (IMR index from CMAP precipitation and NINO3 from Reynolds SST). Similar analysis using RCs corresponding to first two persistent modes (RCs 1 and 2) and the 100-day oscillatory mode (RC34) from CFST62 run ((b); red, green and blue curves).

7. Summary

The dominant daily modes of the south Asian summer monsoon rainfall in the CFS are identified using the technique of the MSSA. The CFST62 has two dominant intraseasonal modes with periods 100 and 30 days. The 100-day mode has northeastward propagation and is similar to the 45-day mode found in observations. The 30-day mode propagates northwestward and can be considered the model equivalent of the 28-day mode seen in observations. Although the structure and behavior of the intraseasonal modes compare well with the observations, the dominant intraseasonal oscillation in CFS is considerably slower and extends well beyond the JJAS summer season. Out of the four persistent components analyzed, three of them are likely to be ENSO-related. The remaining persistent component shows strong links with the eastern Pacific SST, but has positive correlations over there. The impact of the horizontal resolution and the air sea coupling are examined briefly by performing the same analyses on a T126 version of the CFS and its atmospheric model (GFST62) respectively. While no noticeable differences were found between CFST62 and CFST126, the coupled models appear to have more realistic simulation of the oscillatory and persistent modes than the uncoupled one.

References

Krishnamurthy, V., and J. Shukla 2007: Intraseasonal and seasonally persisting patterns of Indian monsoon rainfall. *J. Climate*, **20,** 3-20.

Krishnamurthy, V., and J. Shukla, 2008: Seasonal persistence and propagation of intraseasonal patterns over the Indian monsoon region. *Clim. Dyn.*, **30**, 353-369.

Krishnamurthy, V., and B. Kirtman, 2008: Relation between Indian monsoon variability and SST. *COLA Technical Reports.* 261.

Pegion, K**.,** and B. P. Kirtman, 2007: The Impact of Coupled Air-Sea Interactions on the simulation of Tropical Intraseasonal Variability. Submitted to *J. Climate*.

Plaut, G., and R. Vautard, 1994: Spells of low frequency oscillations and weather regimes in the Northern Hemisphere. *J. Atmos. Sci*., **51,** 210-236

Saha, S. Nadiga, C. Thiaw, J. Wang, W. Wang,Q. Zhang, H. M. van den Dool, H.-L. Pan, S. Moorthi, D. Behringer, D. Stokes, M. Pena, S. Lord, G. White, W. Ebisuzaki, P. Peng, P.Xie , 2006: The NCEP Climate Forecast System. *J.Climate*, **19,** 3483 – 3517.